NASA TECHNICAL MEMORANDUM

NASA TM X-71453

NASA TM X-71453

NOZZLE GEOMETRY AND FORWARD VELOCITY EFFECTS ON NOISE FOR CTOL ENGINE-OVER-THE-WING CONCEPT

by U. von Glahn, J. Goodykoontz, and J. Wagner
Lewis Research Center
Cleveland, Ohio 44135

TECHNICAL PAPER proposed for presentation at Eighty-sixth Meeting of the Acoustical Society of America
Los Angeles, California, October 30- November 2, 1973

NOZZLE GEOMETRY AND FORWARD VELOCITY EFFECTS ON NOISE FOR CTOL ENGINE-OVER-THE-WING CONCEPT

by U. von Glahn, J. Goodykoontz, and J. Wagner

Lewis Research Center

ABSTRACT

Acoustic shielding benefits for jet noise of engine-over-the-wing for conventional aircraft (CTOL) application were studied with and without forward velocity for various small-scale nozzles. These latter included convergent, bypass and mixer, with and without forward ejector, nozzles. A 13-inch free jet was used to provide forward velocity. Far-field noise data were obtained for subsonic jet velocities from 650 to 980 ft/sec and forward velocities from zero to 260 ft/sec. The studies showed that although shielding benefits were obtained with all nozzles, the greatest benefits were obtained with mixer nozzles. The absolute magnitude of the jet noise shielding benefits with forward velocity was similar to the variation in nozzle-only noise with forward velocity.

E-7730

INTRODUCTION

A partial solution that can help to meet acceptable community noise standards for future conventional takeoff and landing (CTOL) aircraft is to place the engine over the wing (EOW) as shown schematically in figure 1. With such an engine-airframe configuration the wing shields the ground observer from much of the high-frequency components of engine noise during flyover and redirects it above the aircraft. When the EOW concept is applied to CTOL aircraft, either or both fan-inlet and engine exhaust (fan and core) noise can be attenuated by a suitable placement of the engine with respect to the wing upper surface.

Noise sources associated with CTOL-EOW configurations are illustrated in figure 2. The most prominent noise source, other than jet exhaust noise, appears to be trailing edge noise from the exhaust flow over the wing. This latter noise source, based on powered-lift configuration studies, is a low-frequency noise source.

For the purpose of attenuating jet exhaust noise, a CTOL-EOW configuration differs from a powered-lift EOW configuration (refs. 1 through 7) in that the jet exhaust flow is not required to attach to the wing surface. Consequently, in order to minimize or eliminate the low frequency surface scrubbing and trailing edge noise sources associated with powered-lift EOW configurations, the engine (hence, jet exhaust nozzle) can be placed some distance above the wing surface (fig. 1). In addition, unconventional nozzles, such as mixer-types, can be utilized in efforts to maximize jet noise attenuation through wing shielding benefits. Such nozzles, in general, generate jet noise at higher frequencies than conventional circular nozzles; therefore the noise attenuation provided by a wing for these higher frequencies may show substantial improvement.

Finally, in order to predict inflight nozzle-wing noise, the forward velocity effects on the aircraft noise level must be established. The ability to predict this noise level is important in determining the approach and takeoff flight paths for minimum aircraft noise over a community. The shielding effectiveness of a wing for CTOL-EOW configurations, therefore, must be established as a function of forward velocity in order to expedite such predictions.

The present study, conducted at the NASA Lewis Research Center using small-scale models, was directed at the following two primary objectives: (1) to evaluate the CTOL-EOW wing shielding effectiveness for various nozzle geometries and (2) to evaluate the forward velocity effect on these nozzle-wing configurations. The nozzle geometries included: (1) convergent circular nozzle, (2) bypass-type (2-stream) nozzle, (3) 6-and 8-tube mixer nozzle and (4) 6-tube mixer nozzle with ejector. The equivalent diameters of the nozzles ranged from 1.56 to 2.9-inches. The acoustic performance of most of these nozzles without a wing is given in reference 8. In the present study, a 13-inch chord wing was used and, except for specific tests, the core nozzle exhaust plane was located at a nominal 20-percent of chord.

A free jet and a stationary microphone arena was used to obtain acoustic data. Use of this technique can cause refraction problems due to the shear layers between the nozzle exhaust jet and free jet as well as the free jet and ambient surrounding. Because cold flow was used for both flow systems, the refraction effect should be minimal. Consequently, the acoustic results presented herein are considered valid and representative of inflight noise characteristics.

Precise predictions for the latter case must, however, include accounting for Doppler shifts in frequency and amplitude.

Acoustic results are presented, for the most part, in terms of spectral data with some consideration being given to noise radiation patterns and sound power level. These data were obtained over a range of nominal jet exhaust velocities from 650 to 980 ft/sec and forward velocities from 0 to 260 ft/sec. Comparisons of the acoustic shielding effects on jet exhaust noise due to a wing are made for the various nozzle geometries tested.

APPARATUS

Acoustic Test Stand

Free jet.- An outdoor 13-inch diameter free jet (fig. 3) was used to simulate forward velocity. For this rig, dry cold air (at about 520° R) was supplied to a 16-inch diameter gate valve from the Center's 125 psig air supply system by way of a 24-inch diameter underground pipe line. A 10-inch diameter butterfly valve was used to control the flow. The nozzle centerline was 12 3/4-feet above the ground.

A muffler system installed in the line downstream of the flow control valve attenuated internal noise caused primarily by the flow control valve. Essentially, the muffler system consisted of perforated plates and dissipative type mufflers. The first perforated plate was located immediately downstream of the flow control valve (40-percent open area plate, 1-in. diameter holes). The other perforated plates were located at the entrance and exit of the first dissipative mufflers (20-percent open area plates, 1/8-in. diameter holes). Both dissipative mufflers were sections of pipe that contained splitter plates oriented at right angles to one another so that the flow divided into four channels. The internal surfaces of the muffler pipes and the surfaces of the splitter plates were covered with 1-in.-thick acoustic absorbent material. The second dissipative muffler was located downstream of the last 45° elbow in the airflow line to take advantage of the reflections caused by turning the flow. In addition the system was wrapped externally with fiber glass and leaded vinyl sheet to impede direct radiation of internal noise through the pipe wall. Two screens (5/16-in. mesh) were placed in the air line downstream of the last muffler to improve the flow distribution to the nozzle.

Test nozzle flow system.- The flow system for the test nozzle, proceeding downstream, consisted of a flow control valve, two perforated plates, a four-chamber-baffled muffler, a 4-inch inlet pipe and, finally, the test nozzle. This muffling system removed sufficient internal noise so that it was not significant in the measured far-field noise levels. Pressurized air was supplied at a nominal temperature of about 520° R.

Models

Wing.- A symmetrical 13-inch chord wooden wing was used in the present study. The wing span was 24-inches. This wing section closely represented that used in references 1 and 2 for a flaps retracted configuration.

Nozzles.- The nozzles tested consisted of four basic types commonly considered for or used with aircraft propulsion systems. They were: (1) convergent circular nozzle, (2) 6-and 8-tube mixer nozzles, (3) 6-tube mixer nozzle with ejector and (4) bypass nozzle. The nozzles were mounted on the free jet centerline. Pertinent nozzle dimensions are given in figure 4 (see also ref. 8). The secondary flow for the bypass nozzle was varied by the insertion of screens upstream of the bypass exhaust plane. Sketches of the location of the nozzles relative to the wing are shown in figure 5. The core nozzle exhaust plane was located at a nominal 20-percent of the wing chord and some distance above the wing surface, except for two special cases.

In the first exception, the convergent circular nozzle lip was placed within approximately 0.4375-inches of the wing surface, at the 20-percent chord station in order to evaluate briefly the effect of vertical displacement of the nozzle exhaust flow on the acoustic shielding of a CTOL configuration. In the second exception (fig. 5(e)), the bypass secondary exhaust plane was placed at the 20-percent chord location and the core exhaust plane was allowed to move downstream but was still afforded some wing shielding.

Data for the 6-tube mixer nozzle with ejector were obtained with the ejector inlet lip located at two stations, 1 5/8-inches downstream and 7/8-inch upstream, relative to the mixer nozzle exhaust plane. These stations correspond, respectively, to the location for maximum thrust augmentation for this ejector and a location that yields additional shielding and absorption capability for a possible acoustically lined ejector while still providing thrust augmentation.

For these two stations the thrust was augmented by 16-percent for the rearward ejector location and 7-percent for the forward location (ref. 8).

Photographs showing typical nozzle-wing configurations mounted in the free jet are shown in figure 6.

PROCEDURE

Data were obtained at nominal jet velocities (test nozzle) from 650 to 980 feet per second. Free jet velocities of 0 to 260 feet per second were used. Sharp-edged orifice plates with appropriate differential pressure taps and thermocouple probes were used to measure airflow for the nozzle flow system. Nozzle total pressures were measured by total pressure tubes upstream of the respective nozzle exhaust planes. Exhaust velocities were calculated by the isentropic equation using total-to-atmospheric pressure ratios and the total temperatures of the flowing air.

Acoustic data were taken with 0.5-inch condenser microphones placed on a 10-foot radius circle centered at the nozzle exit (fig. 7). The microphone horizontal plane and jet centerline were located 12 3/4-feet above the ground. The sound data were analyzed by a 1/3-octave band spectrum analyzer. The analyzer determined sound pressure level (SPL) spectra referenced to 0.0002 microbar. Overall sound pressure levels (OASPL) were computed from the SPL data. The sound power level spectrum and total sound power were computed by special integration of the SPL data from each microphone.

Because the azimuthal noise distribution is not axisymmetrical for a nozzle-wing configuration, the integration required for sound power level spectrum cannot be evaluated directly. Instead a measure of the power spectrum, herein called effective sound power level (PWL'), was computed from the data measured in a single plane (ref. 9). The total sound power was similarly arrived at and is consequently a measure of total sound power, herein called effective total sound power (PWL_T'), rather than an absolute value. Thus, the sound power data herein serve mainly as a guide rather than as absolute values.

No corrections were made to the data for ground reflections. Most of the cancellations and reinforcements in the data occurred at much lower frequencies than the peak noise and are not pertinent to the present study.

FREE JET ACOUSTIC CHARACTERISTICS

Typical sound pressure level spectra below the wing (acoustic radiation angle, 90°) for the 13-inch free jet with the convergent circular nozzle in place but inoperative and with and without the wing are shown by the circle and squate symbols, respectively, in figure 8. The data shown are for a free jet velocity of 175 ft/sec. Also shown in figure 8 are the spectra with the convergent circular nozzle operative at a jet velocity of 970 ft/sec and with a forward velocity of 175 ft/sec. Below a frequency of about 400 Hz, the free jet is acoustically dominant. At frequencies above 400 Hz, sufficient separation (10 dB or greater) exists between the nozzle-wing noise data and that of the free jet to provide valid nozzle-wing noise measurements. With decreasing nozzle jet velocities, the acoustic separation became less. With further decreases in nozzle jet velocity, the acoustic separation becomes less than that shown, until insufficient acoustic separation between the two flows is reached to provide usable noise data. Operation of the free jet at velocities less than 260 ft/sec resulted in a decrease in the free jet sound pressure level. Thus, a wide range of useful combinations of the test nozzle and free jet velocities were available for the present work. In general, nozzle-only and nozzle-wing noise data separated from the free jet noise level by at least 10 dB and above 400 Hz only are included in this report.

ACOUSTIC SHIELDING

In this section of the report, the overall acoustic trends are discussed that provide the baseline information necessary for an understanding of the possible jet noise attenuation by the engine-over-the-wing concept. The noise caused by the nozzle-only exhaust flow is the base from which acoustic shielding benefits are measured.

General

In general, the jet exhaust noise below the wing at acoustic radiation angles between 70° and 120° measured from the inlet is of most interest for community noise considerations. For the most part, only the noise below the wing at 90° will be discussed. Since the acoustic trends at this angle are considered representative of those at the radiation

angles of interest. Except as noted, the data presented will be for a nominal jet exhaust velocity of 940 ft/sec. Acoustic data at radiation angles and jet exhaust velocities other than these just mentioned will be discussed only to illustrate specific points or to confirm acoustic scaling laws. The acoustic characteristics discussed include sound pressure level (SPL) and sound power level (PWL') spectra, overall sound pressure level (OASPL) and total sound power (PWL_T').

Acoustic scaling laws and general acoustic trends associated with the engine-over-the-wing concept are summarized briefly in the following section. The data presented are limited to the convergent circular nozzle with and without a wing. The data trends presented are representative of the other nozzles and nozzle-wing configurations tested.

Nozzle-only.- In reference 8 and others, it has been shown that the sound pressure level characteristics of nozzle-only jet exhaust noise generally scale according to the Strouhal relation given by fD_e/U_j for static external flow conditions (zero forward velocity).

With forward velocity, both the sound pressure level and the sound power level for the nozzles are attenuated from the levels measured for static external flow conditions. This attenuation is discussed in detail in reference 8 and methods for its estimation are given.

Shielding of jet noise by wing.- When a wing is placed below the jet exhaust nozzle to provide jet noise attenuation, as with an EOW configuration, the noise above the wing is amplified by acoustic reflections from the wing surface. The jet noise below the wing is attenuated over a wide range of acoustic radiation angles (ref. 7). The attenuation principles involved are generally similar to those associated with erecting barriers for controlling noise sources on the ground.

A representative example of acoustic amplification and attenuation for an EOW configuration with a convergent circular nozzle is shown in figure 9 for acoustic radiation angles directly above (270°) and below (90°) the wing. (The nozzle-wing configuration used to obtain these data is shown in figure 5(a).) In the figure, the sound pressure level spectra data are shown for a nominal jet exhaust velocity of 940 ft/sec. Also shown, for comparison, is the nozzle-only spectral curve. At a Strouhal number greater than 1.0, above the wing acoustic amplification of 1-2 dB occurred; below the wing an acoustic attenuation of up to 6 dB was obtained.

A typical increase in noise above the nozzle-only data, herein called jet-wing interaction noise, also is evident in the low frequency range in figure 9. This additional noise is caused by the nozzle exhaust flow scrubbing a portion of the wing surface and the shear layer noise caused by the flow at the trailing edge of the wing.

Except as noted, hereinafter only acoustic data below the wing will be presented.

Nozzle height above wing.- The amount of jet-wing interaction noise at the low frequencies shown in figure 9 is small because the nozzle was mounted at an appreciable height above the wing surface (fig. 5(a)). Consequently, only a small portion of the spreading circular-nozzle exhaust plume came into contact with the wing surface and trailing edge to cause the interaction noise. When the same nozzle was placed close to the wing surface (within 0.45 in.) herein called "on-wing", the low frequency noise generation is increased significantly, as shown in figure 10, by the increased wing surface scrubbed by the jet exhaust plume and the greater trailing edge region affected by this jet flow. The shielding of the jet exhaust noise by the wing at high frequencies appears to be the same at both nozzle locations. However, the intersection of the nozzle-only spectral curve by the nozzle-wing configuration spectral data occurs at a slightly higher frequency when the nozzle is not near the wing surface; herein called "off-wing."

Shielding Effectiveness

A convenient method of presenting the effect of wing shielding on jet exhaust noise is in terms of the SPL difference between the nozzle-wing configuration and the nozzle-only, $(SPL-SPL_N)$, as a function of Strouhal number. The $(SPL-SPL_N)$-term herein is defined as the acoustic shielding effectiveness (ASE) parameter. Positive values of this parameter denote jet-wing interaction noise above the nozzle-only noise. Negative values of the parameter denote jet noise shielding by the wing.

The ASE-parameter values as a function of Strouhal number are shown in figures 11 to 18 for the nozzle-wing configurations tested. The data are presented at a radiation angle of 90°, except as noted, and with and without forward velocity.

Zero forward velocity.- The shielding effectiveness of the wing with the convergent circular nozzle in terms of the ASE-parameter as a function of Strouhal number is shown by the data in figure 11. The data given are for nominal jet exhaust velocities from 680 to 970 ft/sec. The acoustic data correlate to a single curve with Strouhal number in the region where the jet exhaust noise is shielded by the wing. With the off-wing nozzle location jet noise shielding at Strouhal numbers greater than 0.4 (1600 to 2500 Hz for the model configuration, with the lowest frequency associated with the lowest jet velocity). The maximum jet noise suppression due to wing shielding occurs at the highest Strouhal number and amounts to about 6 dB. The attenuated jet SPL data due to the shielding of the wing correlates in the same manner as the nozzle-only data; i.e., 8-power velocity law.

The jet-wing interaction noise becomes increasingly more dominant with decreasing jet velocities compared with the nozzle-only noise. This results in the higher positive values of shielding effectiveness parameter with decreasing jet exhaust velocities as shown in figure 11(a).

With the on-wing nozzle location (fig. 11(b)), the shielding of the jet noise by the wing is delayed to a somewhat higher Strouhal number of about 0.5 (3-4000 Hz compared to 1600-2500 Hz for the off-wing location). At Strouhal numbers greater than 1.0, however, the ASE-parameter values appear to be substantially independent of nozzle location above the wing surface for the range included herein. A comparison of the jet-wing interaction noise (positive values of the shielding effectiveness parameter) shows that this noise is about 5 dB greater for the on-wing than that for the off-wing nozzle location because of greater amounts of scrubbing and trailing edge noise generated when the jet is close to the wing surface.

The jet-wing interaction noise is not correlated by the Strouhal number as is obvious in figure 11. The relation of the jet-wing interaction noise is a lower (6-power) function of jet velocity compared with that for jet exhaust noise shielding and nozzle-only noise (8-power). Furthermore, the jet-wing interaction noise is composed of noise sources separate from the jet noise source and is a function of the flow velocity scrubbing the wing surface and the velocity at the wing trailing edge. Consequently, it is of no surprise that a different correlation from that for jet noise shielding is required for these additional noise sources. Such a

correlation is beyond the scope of this study and as will be discussed later may be of no interest for large scale noise applications.

Trends similar to those discussed for the convergent-circular nozzle-wing configuration were also observed with the other nozzle-wing configurations tested. The absolute magnitudes of jet noise shielding and the Strouhal numbers at which shielding began, however, varied with the specific nozzle-wing configuration. These variations will be discussed to some extent in a later section that deals with the effect of forward velocity on the ASE-parameter.

Acoustic radiation angle.- The effect of acoustic radiation angle on the ASE-parameter for a convergent-circular nozzle-wing configuration is shown in figure 12 for zero forward velocity and a nominal jet velocity of 940 ft/sec. In general, the acoustic shielding is somewhat reduced with an increase in radiation angle from 90° to 120°. A difference in trend between the on-wing and off-wing nozzle locations occurs at 140°. At this angle, the on-wing nozzle location shows a maximum shielding whereas the off-wing nozzle location shows a minimum shielding. This trend difference is caused by the particular flow conditions existing on the wing surface for the specific nozzle-wing configurations. The jet-wing interaction noise (Strouhal number < 0.5) is reduced for both nozzle locations with an increasing radiation angles from 90° to 140°.

Representative sound pressure level spectral data are shown for the 6-tube mixer nozzle in figure 13 for acoustic radiation angles from 80° to 140°. In general, these data show substantially the same shielding effectiveness for 80° to 100°. For radiation angles from 100° to 140°, the acoustic shielding effectiveness is rapidly reduced with increasing radiation angles. In comparison with the circular nozzle data (fig. 12) the mixer nozzle-wing configuration, in general, shows more shielding but also more low frequency interaction noise.

The other nozzle-wing configurations tested showed noise trends with acoustic radiation angles similar to those for the 6-tube mixer nozzle.

Forward velocity.- The effect of forward velocity on the acoustic shielding effectiveness parameter is shown in figures 14 to 18 for the nozzle-wing configurations tested. The data are shown as a function of Strouhal number for a nominal jet velocity of 940 ft/sec and forward velocities from zero up to

260 ft/sec. In general, no significant effects (less than 3 dB) with forward velocity are noted for the region in which the jet exhaust noise is shielded. This indicates that with forward velocity, the shielded jet noise generally behaves substantially in the same manner as pure jet exhaust noise. Similar results were obtained at lower jet exhaust velocities (680 and 835 ft/sec).

On the basis of the data shown in figures 14 through 18, it is apparent that the largest amounts of jet exhaust noise shielding by the wing were provided with the mixer-type nozzles (figs. 15 and 16). The data also show in figure 17 that with a mixer nozzle and ejector configuration, additional acoustic shielding by the wing was evident at low frequencies compared to the same mixer nozzle without an ejector (fig. 17). Jet exhaust noise shielding with a bypass nozzle and wing shielding (fig. 18) extends over about the same range of Strouhal numbers as those for a convergent circular nozzle and wing (fig. 14). However, the bypass nozzle-wing configuration, for the most part, did not achieve the same magnitude of jet exhaust noise suppression as that with the convergent-circular nozzle-wing configuration.

With increasing forward velocity the jet-wing interaction noise (low frequency range), in general, is increasingly reduced for both the on-wing and off-wing nozzle locations. A deviation from this trend is noted in the on-wing data (fig. 14) in the range of Strouhal numbers from 0.16 to 0.6. It is believed that these data are still associated with the jet flow on the wing whereas the data below a Strouhal number of 0.16 appears to be associated with the flow off the wing trailing edge. These latter data then do not appear to correlate in the same manner with the nozzle-only SPL values for forward velocity (ref. 8).

The 6-tube mixer nozzle with ejector configurations (fig. 17) also show no significant effect of forward velocity on jet-wing interaction noise. It is believed that this acoustic behavior is peculiar to the specific configuration.

OVERALL NOISE VALUES

Sound Pressure Level

Zero forward velocity.- A representative acoustic radiation pattern with zero forward velocity is shown in figure 19

for a nozzle-only and nozzle-wing configuration. The OASPL data shown are for the 6-tube mixer nozzle with a nominal jet exhaust velocity of 940 ft/sec. As previously noted, the noise above the wing is somewhat louder for the nozzle-wing configuration than that for the nozzle-only. Below the wing, particularly at the radiation angles of interest (70° to 120°) the jet exhaust noise is substantially reduced by the presence of the wing. These results are generally representative of the other nozzle-wing configurations tested. Exceptions did occur for some configurations when the jet-wing interaction noise was sufficiently large to dominate the jet exhaust noise, even with shielding benefits at high frequencies. Some of these exceptions and their significance are discussed in the next section dealing with forward velocity effects on OASPL values.

Forward velocity.- OASPL variations as a function of acoustic radiation angle are shown in figure 20 for several representative nozzle-wing configurations tested. The data shown are for a nominal jet exhaust velocity of 940 ft/sec and forward velocities from zero up to 260 ft/sec. The acoustic data are plotted in terms of the OASPL difference between the nozzle-wing configuration and the nozzle-only. Positive values of this OASPL-parameter indicate noise increases, while negative values indicate noise suppression compared with the nozzle-only case. Positive values for the OASPL parameter are caused by large magnitudes of jet-wing interaction noise that dominates any shielding of jet exhaust noise by the wing. The absolute magnitudes of the data are of no particular significance because the importance of the low frequency noise in model tests generally tends to become less important when scaled to full-size. This is due primarily to the acoustic frequency weighting procedures used in computing perceived aircraft noise. However, the data trends shown by the plots in figure 20 are of interest. Generally, in all cases shown, except that for the on-wing nozzle location (solid symbols, fig. 20(a)), the effect of forward velocity is to decrease the OASPL-parameter values (values become less positive or more negative). This effect of forward velocity occurs because the jet-wing interaction noise is decreased by forward velocity rather than due to any improvement in jet exhaust noise shielding by the wing. As previously noted an opposite affect of forward velocity on the OASPL-parameter is noted for the on-wing nozzle location (fig. 20(a)). It is believed that this opposite trend may be a configuration pecularity and/or a phenomena of the exhaust flow attachment to the wing surface.

Sound Power

Sound power level spectra.- The effective sound power level spectra (PWL') for the nozzle-wing configurations with and without forward velocity were not significantly different from those for the nozzle-only at the same operating conditions. When differences did occur, the trend was to increase the sound power level of the nozzle-wing configurations, compared to the nozzle-only, at low frequencies. Such a situation was observed for the 6-tube mixer nozzle configuration shown in figure 21(a). Somewhat larger differences were observed with the 8-tube mixer nozzle configuration (fig. 21(b)). Data in figure 21 are for a jet exhaust velocity of 940 ft/sec and zero forward velocity. In addition, the effective sound power level was somewhat reduced at the high frequencies for the 8-tube mixer nozzle-wing configuration. The effect of forward velocity on PWL' was to afford some reduction in these differences between the nozzle-wing and nozzle-only data (by as much as 1/3 those shown in figure 21(b)).

Total sound power.- The effective total sound power for all the nozzle-wing configurations are shown in figure 22 as a function of jet exhaust velocity and zero forward velocity. The data show that the effective total sound power varies generally with 8-power velocity law when plotted as a function of the jet-exhaust or core velocity. (Only the data for configurations with an ejector showed a tendency toward a lower power velocity law, possibly the 6-power.) Because the effective sound power level spectra for the nozzles with and without a wing were not significantly different, the values shown in figure 22 are substantially the same as those for the nozzle-only in reference 8.

The nozzle-wing configurations showed the same attenuation trends in effective total sound power with forward velocity as did the nozzles-only reported in reference 8.

SHIELDING BENEFITS FOR EQUAL THRUST

In order to assess the absolute benefits of wing shielding associated with various nozzle geometries, the acoustic data herein for the nozzle-wing configurations must be normalized on an equal thrust basis and a common chord size to provide the proper wing-shielding comparison. Normalization of the acoustic data to equal thrust was accomplished by dimensionally scaling the effective nozzle area. All the nozzles were scaled to the calculated thrust level of the

bypass nozzle operating at a secondary to core flow velocity ratio, U_s/U_c, of 0.7. This nozzle provided the largest thrust of all those tested herein. A jet exhaust (or core) velocity of 940 ft/sec was selected for the assessment of the shielding benefits.

When the acoustic data for different nozzle-wing configurations are scaled on the basis of the nozzle size, the effect of the wing is similarly scaled. Consequently, a comparison between the scaled acoustic values is invalid because the shielding effectiveness is a function of the nozzle-to-wing chord size. Thus, when the nozzle size is scaled for equal thrust, the wing size for all nozzles must then be scaled to a common chord size. Unpublished NASA acoustic data on the effect of nozzle-to-wing dimensional changes were used to normalize the nozzle-wing acoustic data herein when the nozzle dimensions were scaled to achieve equal thrust.

Sound Pressure Level

For later use herein, the nozzle-only SPL spectra normalized on an equal thrust basis are shown in figure 23 for an acoustic radiation angle of 90°. Also tabulated on the figure are the OASPL values for the nozzles. It is apparent that the lowest overall sound pressure level is attained with the bypass nozzle operating at a U_s/U_c ratio of 0.5. The highest OASPL level is obtained with the convergent circular nozzle. The difference in SPL spread for the nozzles is nearly 6 dB.

The normalized (equal thrust, constant chord) SPL spectra at an acoustic radiation angle of 90° for the major nozzle-wing configurations are shown in figure 24. The following procedure was used to construct the curves shown. At the frequencies where the jet exhaust noise is shielded by the wing, the normalized shielded (attenuated) data were used; at the frequencies where no shielding of the jet noise by the wing occurred, the normalized nozzle-only data were used. The dividing points between the two sets of data are shown by the triangle symbol in figure 24.

The jet-wing interaction noise evident in the measured data discussed previously was omitted in figure 24 because the level of this noise is a function of nozzle placement vertically above the wing and can be modified without significantly affecting the shielding effectiveness of the wing at the high frequencies. In addition, noise suppression methods could possibly be used (ref. 9) to reduce the jet-wing

interaction noise at low frequencies to perhaps the level of the nozzle-only values. Thus, the curves in figure 24 represent optimized noise goals for the CTOL-EOW configurations tested herein. Also tabulated on the figure are the calculated OASPL values for each configuration. The results of this exercise indicates that the 8-tube mixer nozzle with wing shielding yielded the lowest OASPL. The 6-tube mixer nozzle configuration was a close second. The bypass nozzle was somewhat higher (2-3 dB) than the 8-tube mixer nozzle although its basic shielding effectiveness was not substantial (fig. 18). Its good showing resulted primarily from the large amount of nozzle jet exhaust noise attenuation shown in figure 23. The several versions of the bypass nozzle-wing configurations are presented separately in figure 25 and show that the geometry and operating changes indicated did not significantly affect the absolute noise attenuation. No shift in spectra occurred for the nozzle-wing configurations shown.

Total Sound Power

In order to provide a more pertinent comparison of the effective total sound power for the nozzle-wing configurations, these data also were normalized on an equal thrust basis and constant wing chord and were plotted as a function of jet velocity (fig. 26). The nozzles were dimensionally scaled to the thrust level of the largest nozzle (bypass) with a ratio of U_s/U_c of 0.7. The jet-exhaust or core velocity was fixed constant at 940 ft/sec. It is apparent that the nozzle-wing configuration with the convergent circular nozzle generates the greatest amount of noise and those with the bypass nozzles generate the least noise. The data for the mixer nozzles are about midway between that for these two configurations. The effective total sound power for the nozzle-wing configurations shown in figure 26 would be reduced with forward velocity in substantially the same manner as those for the nozzles-only given in reference 8.

The 6-tube nozzle with ejector is not included in figure 26 because the thrust augmentation varies with forward velocity thus making a simple comparison difficult with those nozzles that do not incorporate this operational phenomena.

CONCLUDING REMARKS

When scaling model data to a full-sized aircraft, the shifts in the peak frequency typical of the various nozzles

(fig. 23) could affect the perceived noise level for an aircraft. However, with the nozzle-wing configurations these shifts in peak frequency are no longer evident (fig. 24). Thus, scaling the present data to a large aircraft would show no significant perceived noise level effects between the nozzle-wing configurations that could be attributed to nozzle geometry. Consequently, trade-offs in aerodynamic and weight-considerations rather than acoustic considerations probably would dictate the selection of the ultimate nozzle-wing configuration.

The jet-wing interaction noise for a full scale CTOL-EOW aircraft may well be a minor noise consideration because the perceived noise weighting at the low frequencies for a full sized aircraft would minimize its noise effect. Suppression means or nozzle location relative to the height of the wing could further alleviate the problem if it should become an annoyance factor. It should be noted, however, that the low frequency noise should be examined to ascertain whether it could cause sufficient structural vibration problems with respect to wing panel or fuselage skin fatigue.

NOMENCLATURE

(English units, except as noted)

D_e	equivalent diameter of total nozzle area
f	1/3 octave band spectrum frequency, Hertz
OASPL	overall sound pressure level, dB
PWL'	effective sound power level, dB re 10^{-13} w
PWL_T'	effective total sound power, dB re 10^{-13} w
SPL	sound pressure level, dB
U_c	core exhaust velocity
U_j	jet exhaust velocity
U_{jc}	jet core velocity
U_o	forward velocity
U_{ref}	reference jet velocity for normalization, 940 ft/sec
U_s	secondary (bypass) exhaust velocity
Subscript:	
N	nozzle

REFERENCES

1. M. Reshotko, W. A. Olsen, and R. G. Dorsch, NASA TM X-68032 (1972).

2. M. Reshotko, W. A. Olsen, and R. G. Dorsch, NASA TM X-68104 (1972).

3. R. G. Dorsch, P. L. Lasagna, D. L. Maglieri, and W. A. Olsen, NASA SP-311 (1972), p. 259.

4. R. Dorsch and M. Reshotko, STOL Technology Conference, NASA SP-320 (1973).

5. R. Dorsch, M. Reshotko, and W. Olsen, AIAA paper 72-1203 (1972).

6. U. von Glahn, M. Reshotko, and R. Dorsch, R. Dorsch, NASA TM X-68159 (1972).

7. M. Reshotko, J. Goodykoontz, and R. Dorsch, AIAA paper 73-631 (1973).

8. U. von Glahn, D. Groesbeck, and J. Goodykoontz, AIAA paper 73-629 (1973).

9. W. A. Olsen, R. G. Dorsch, and J. H. Miles, NASA TN D-6636 (1972).

10. D. Chestnutt, R. Hayden, and D. Maglieri, STOL Technology Conference, NASA SP-320 (1973).

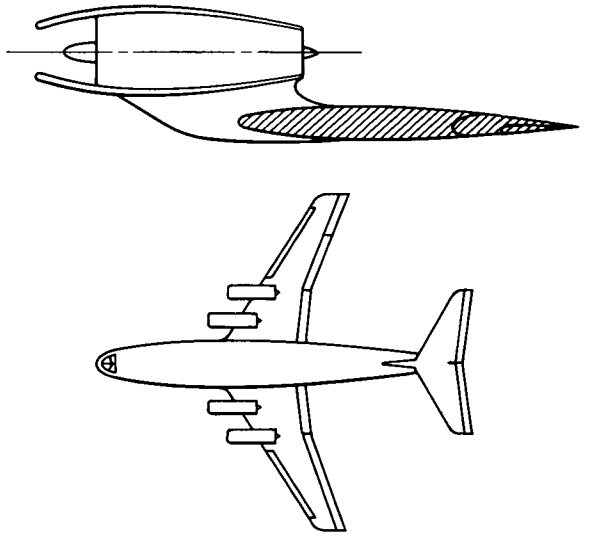

Figure 1. - Schematic of conventional (CTOL) airplane with engine over the wing (EOW).

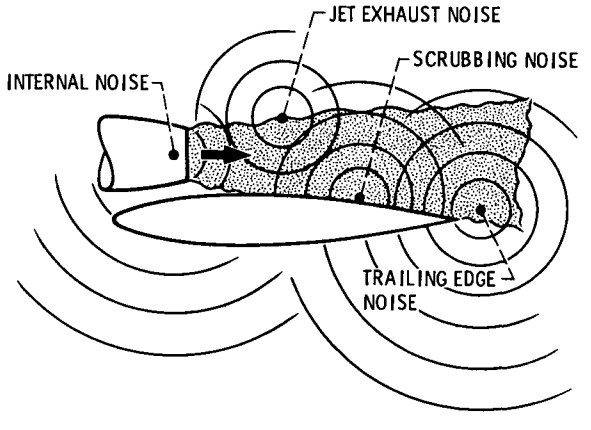

Figure 2. - Noise sources for CTOL - EOW configuration.

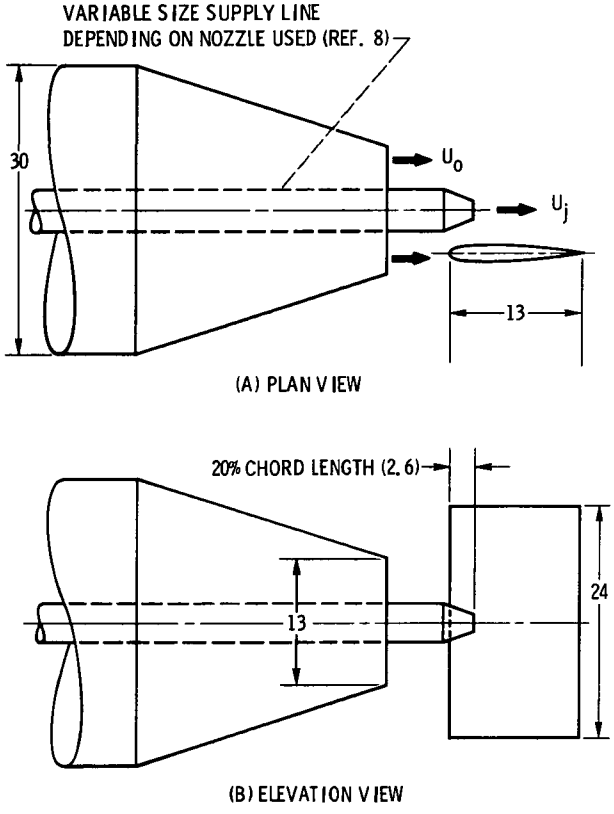

Figure 3. - Schematic of typical nozzle-wing configuration in free jet for acoustic measurements. All dimensions in inches.

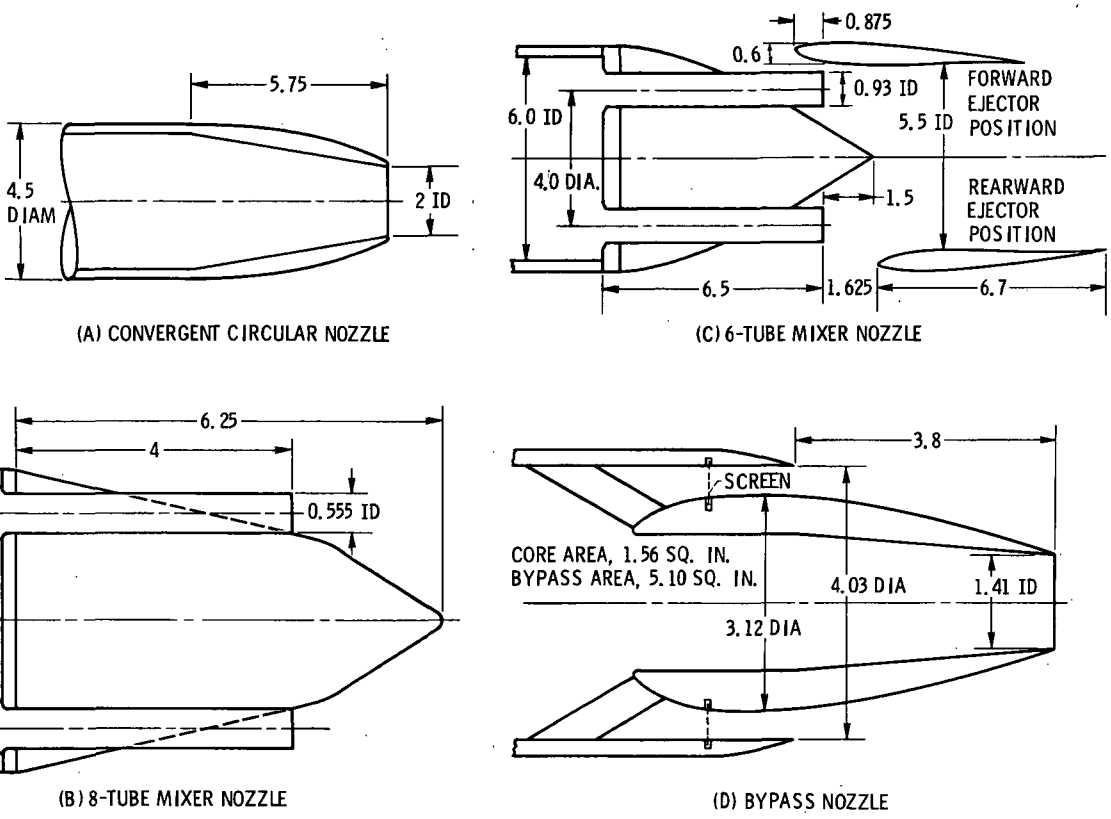

Figure 4. - Nozzle dimensions. (All dimensions are in inches.)

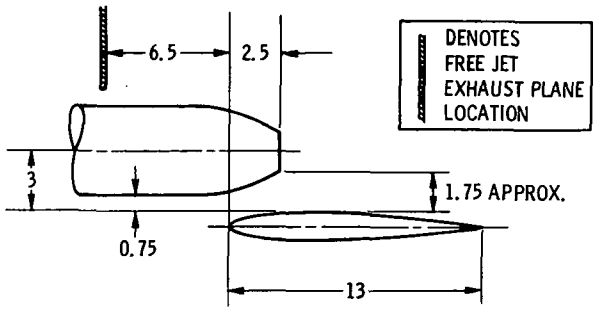

(A) CONVERGENT CIRCULAR NOZZLE

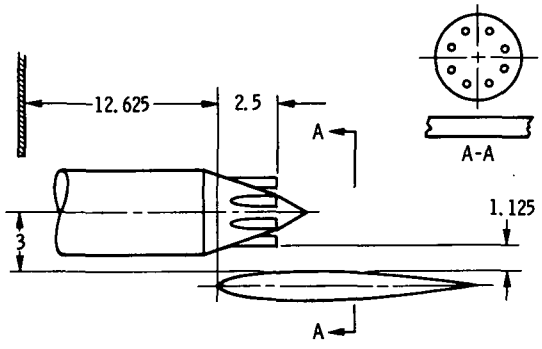

(B) 8-TUBE MIXER NOZZLE

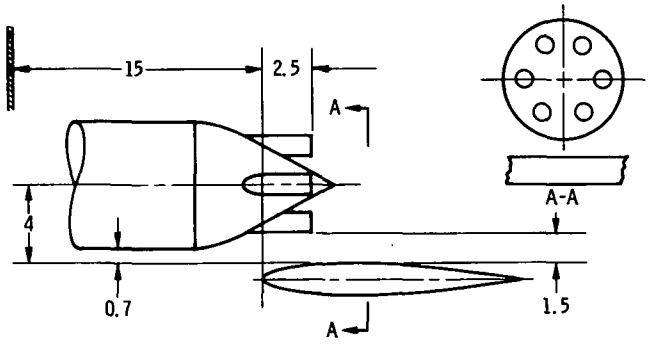

(C) 6-TUBE MIXER NOZZLE.

Figure 5. - Nozzle-wing orientations. (All dimensions are in inches.)

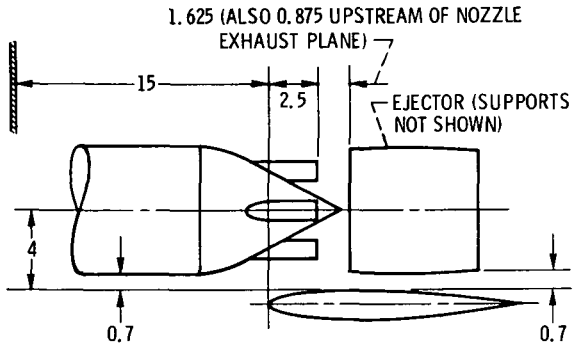

(D) 6-TUBE MIXER NOZZLE WITH EJECTOR.

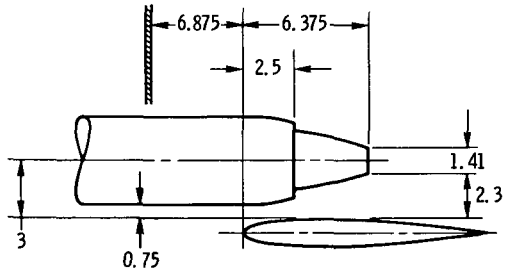

(E) BYPASS NOZZLE; BYPASS EXHAUST AT 20% CHORD

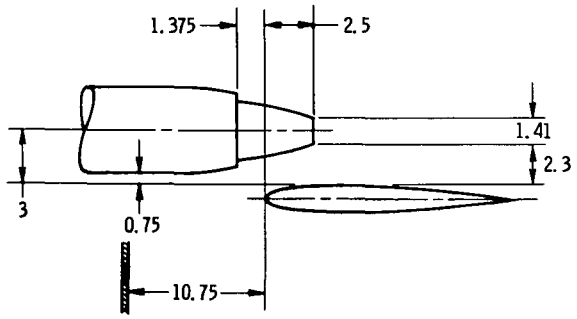

(F) BYPASS NOZZLE; CORE EXHAUST AT 20% CHORD

Figure 5. - Concluded.

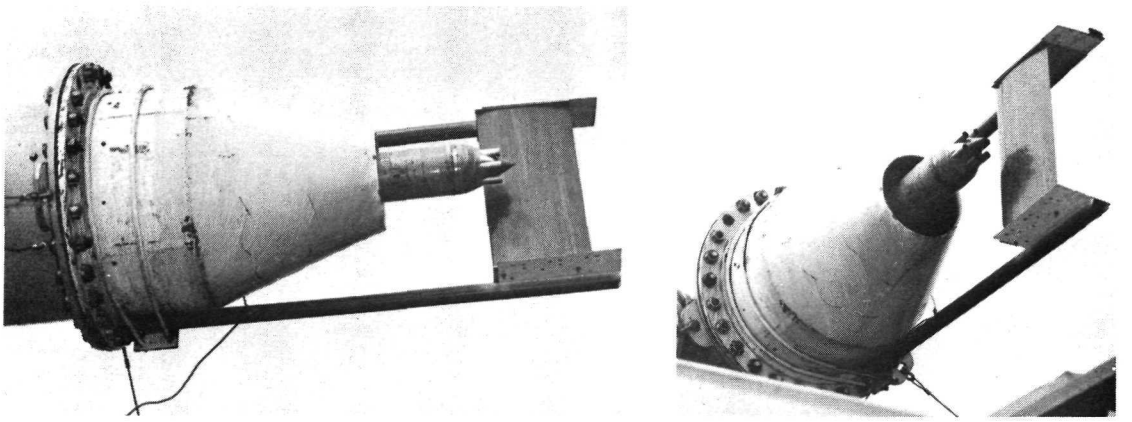

(a) 6-TUBE MIXER NOZZLE WITH WING.

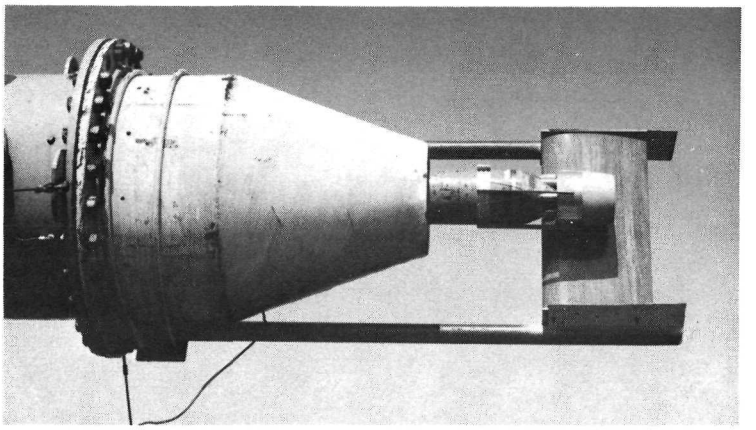

(b) 6-TUBE MIXER NOZZLE WITH EJECTOR AND WING.

Figure 6. - Typical nozzle-wing configurations mounted in free jet.

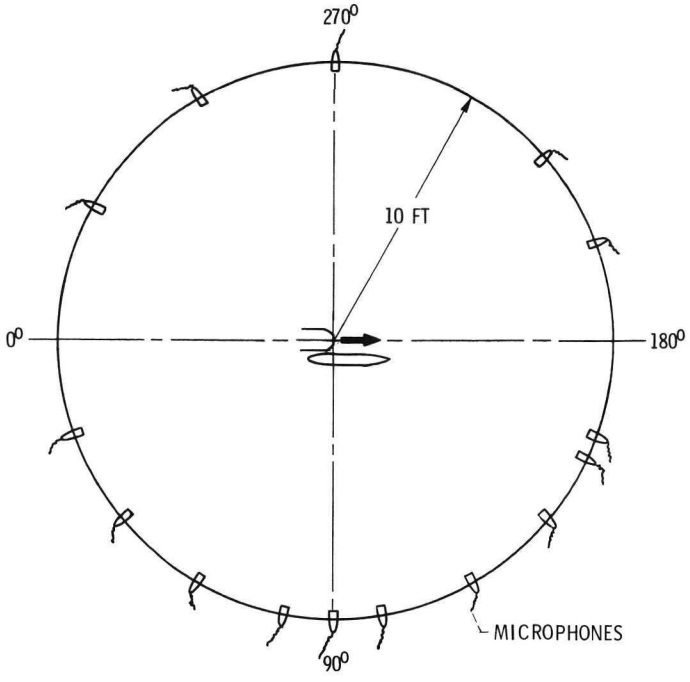

Figure 7. - Typical microphone layout.

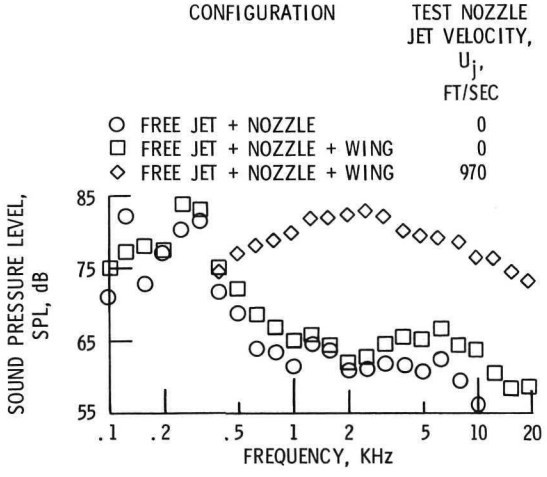

Figure 8. - Typical sound pressure level characteristics of free jet with and without operation of circular nozzle. Free jet velocity, 175 ft/sec; acoustic radiation angle, 90°.

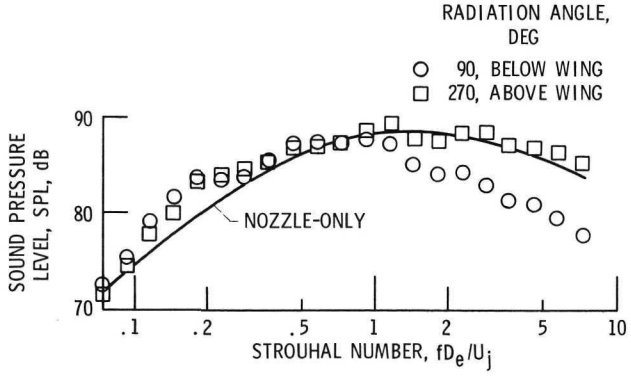

Figure 9. - Acoustic shielding of jet exhaust noise by wing. Convergent circular nozzle; jet exhaust velocity, 940 ft/sec; zero forward velocity.

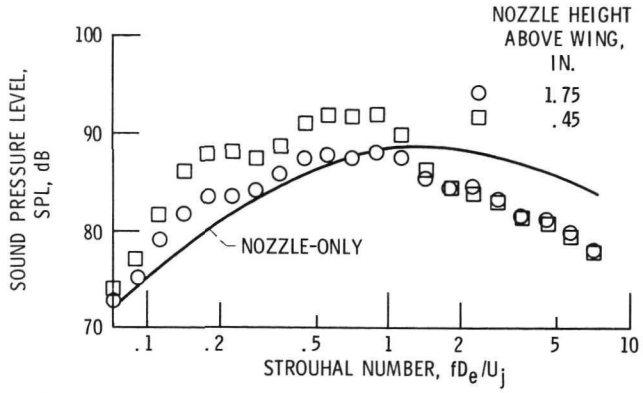

Figure 10. - Effect of nozzle height above wing on acoustic shielding of jet exhaust noise. Convergent circular nozzle; jet exhaust velocity, 940 ft/sec; zero forward velocity; radiation angle, 90^0.

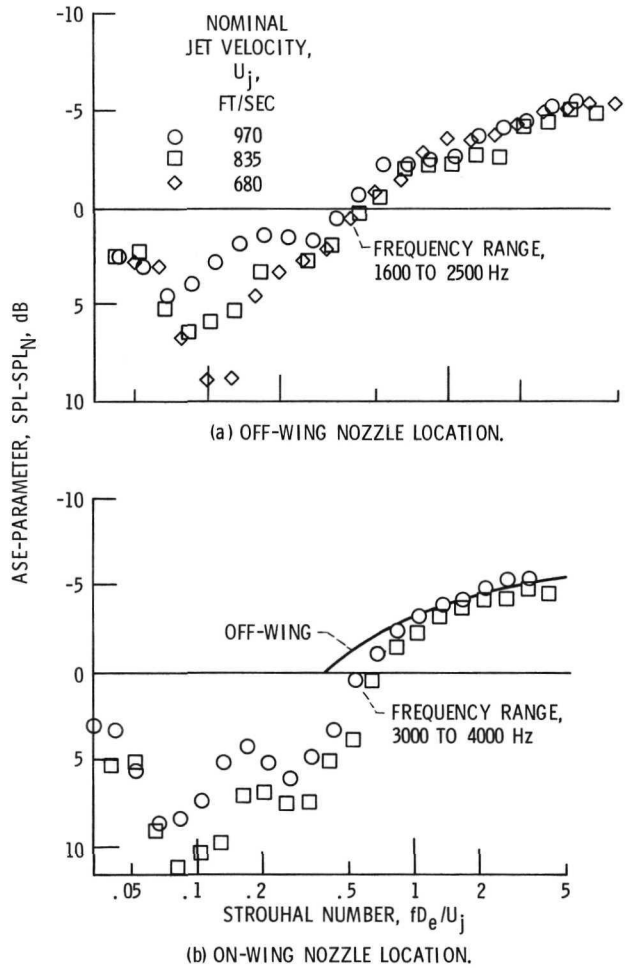

Figure 11. - Typical effect of jet exhaust velocity on acoustic shielding effectiveness parameter as a function of Strouhal number. Convergent circular nozzle; zero forward velocity; radiation angle, 90^0.

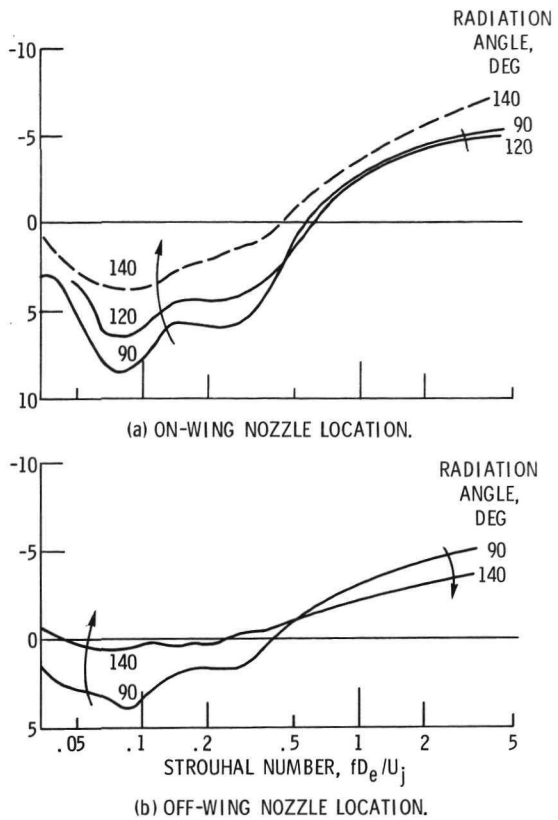

Figure 12. - Effect of acoustic radiation angle on acoustic shielding effectiveness parameter. Convergent circular nozzle; jet exhaust velocity, 940 ft/sec; zero forward velocity.

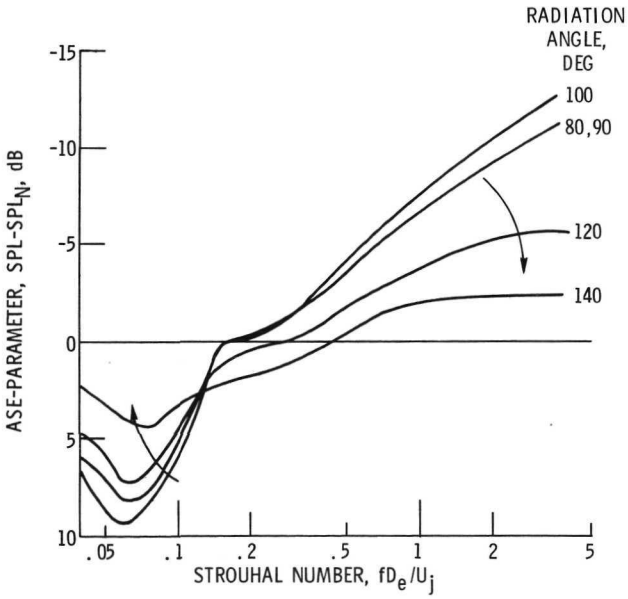

Figure 13. - Effect of acoustic radiation angle on acoustic shielding effectiveness parameter. 6-Tube mixer nozzle; jet exhaust velocity, 940 ft/sec; zero forward velocity.

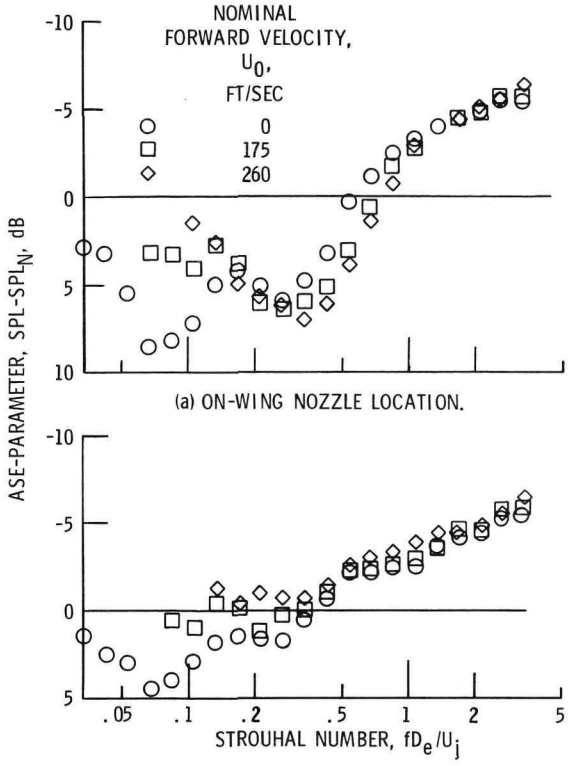

Figure 14. - Effect of forward velocity on acoustic shielding effectiveness parameter. Convergent circular nozzle; nominal jet exhaust velocity, 940 ft/sec; radiation angle, 90°.

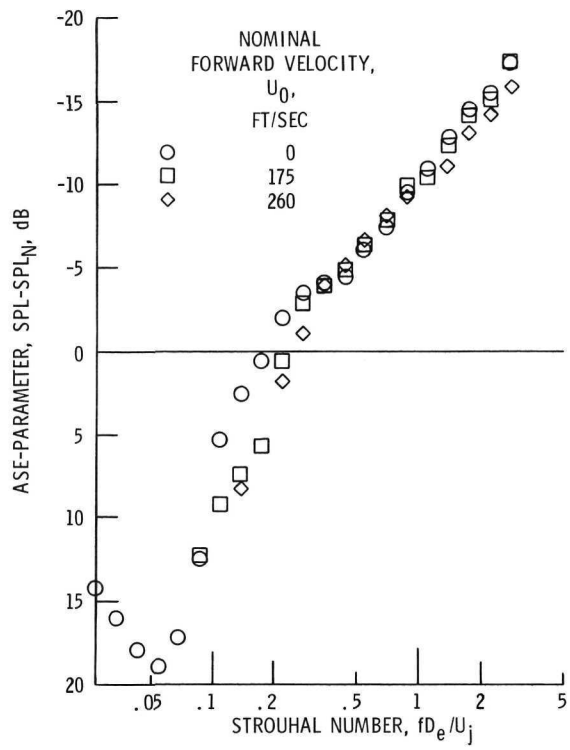

Figure 15. - Effect of forward velocity on acoustic shielding effectiveness parameter. 8-Tube mixer nozzle; nominal jet exhaust velocity, 940 ft/sec; radiation angle, 90°.

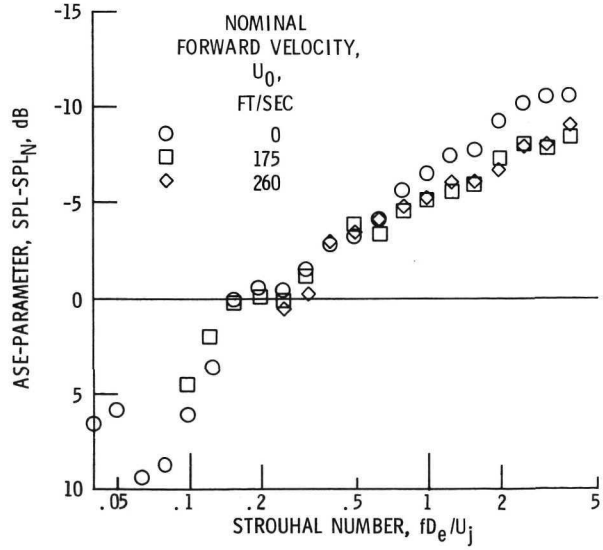

Figure 16. - Effect of forward velocity on acoustic shielding effectiveness parameter. 6-Tube mixer nozzle; nominal jet exhaust velocity, 940 ft/sec; radiation angle, 90°.

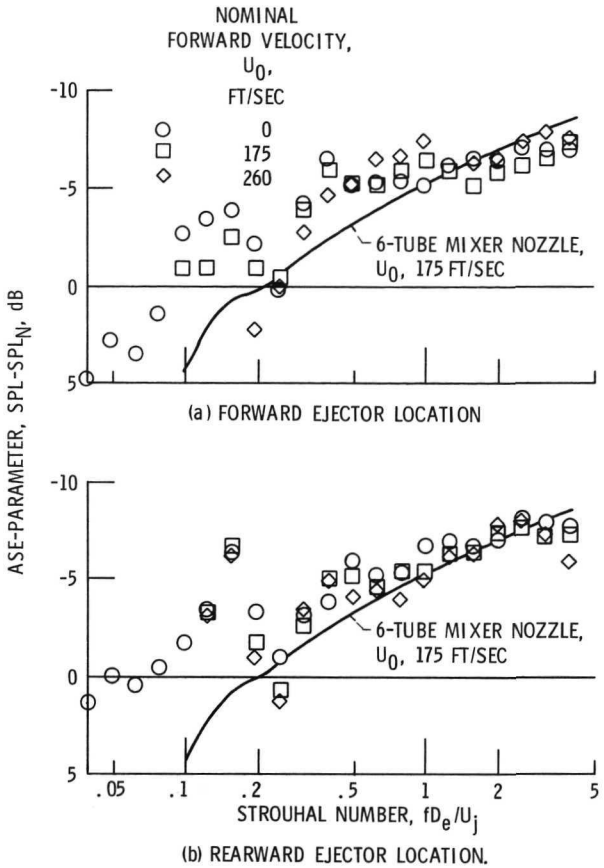

Figure 17. - Effect of forward velocity on acoustic shielding effectiveness parameter. 6-Tube mixer nozzle with ejector; nominal jet exhaust velocity, 940 ft/sec; radiation angle, 90°.

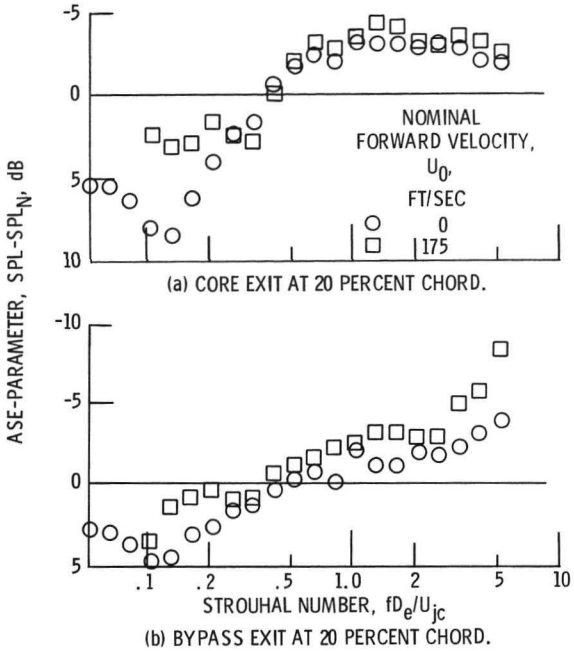

Figure 18. - Effect of forward velocity on acoustic shielding effectiveness parameter. Bypass nozzle; nominal jet core exhaust velocity, 940 ft/sec; U_s/U_c, 0.7; radiation angle, 90°.

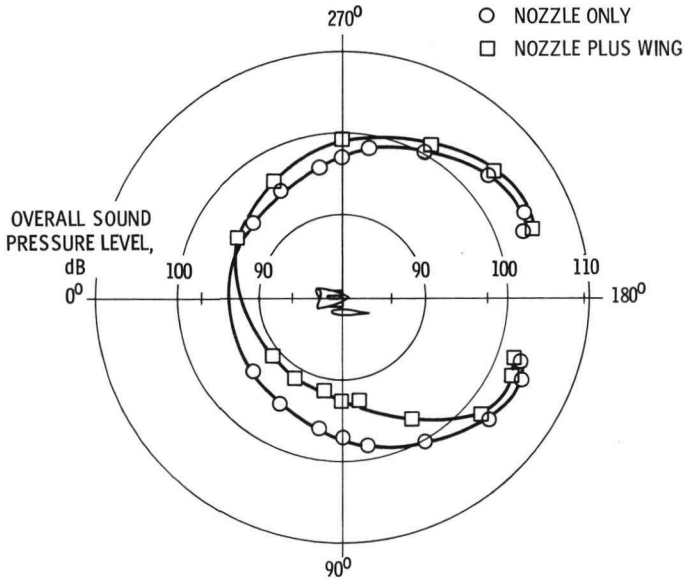

Figure 19. - Typical noise radiation patterns for nozzle-only and nozzle-wing configuration. 6-Tube mixer nozzle; jet exhaust velocity, 940 ft/sec; zero forward velocity.

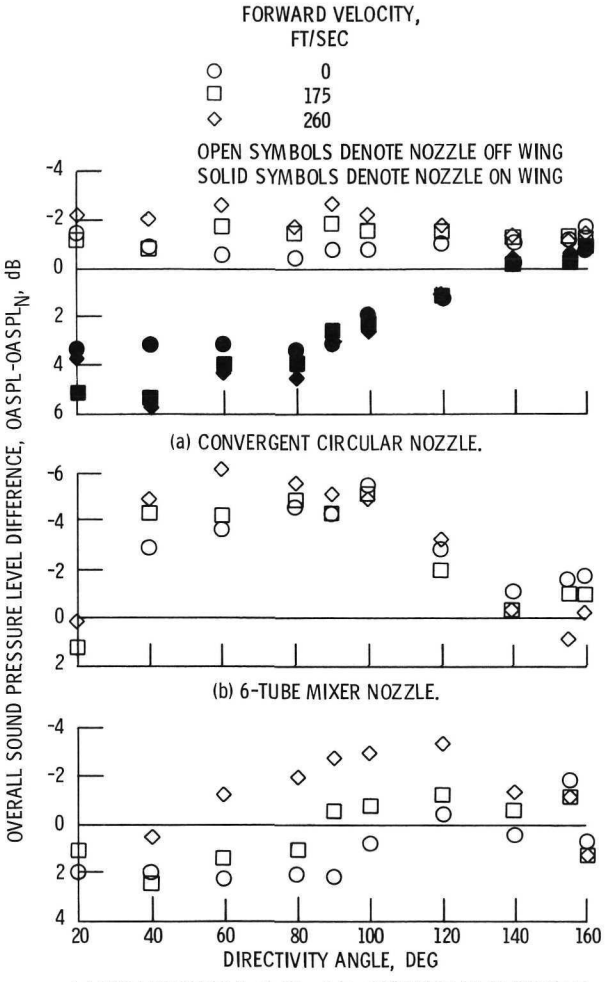

(a) CONVERGENT CIRCULAR NOZZLE.

(b) 6-TUBE MIXER NOZZLE.

(c) BYPASS NOZZLE; U_s/U_c, 0.7; CORE EXIT AT 20 PERCENT CHORD.

Figure 20. - Effect of forward velocity on radiation pattern of typical nozzle-wing configurations. Nominal jet exhaust velocity, 940 ft/sec.

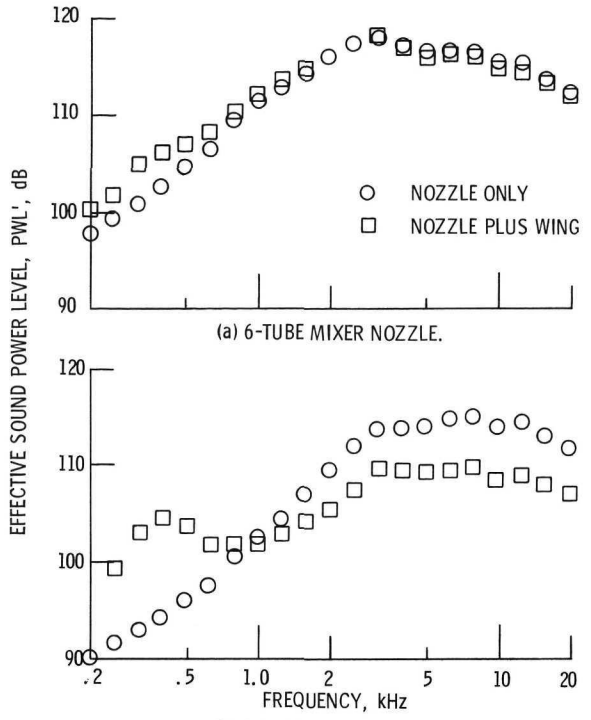

(a) 6-TUBE MIXER NOZZLE.

(b) 8-TUBE MIXER NOZZLE.

Figure 21. - Effect of wing shielding on effective sound power level spectra. Nominal jet exhaust velocity, 940 ft/sec; zero forward velocity.

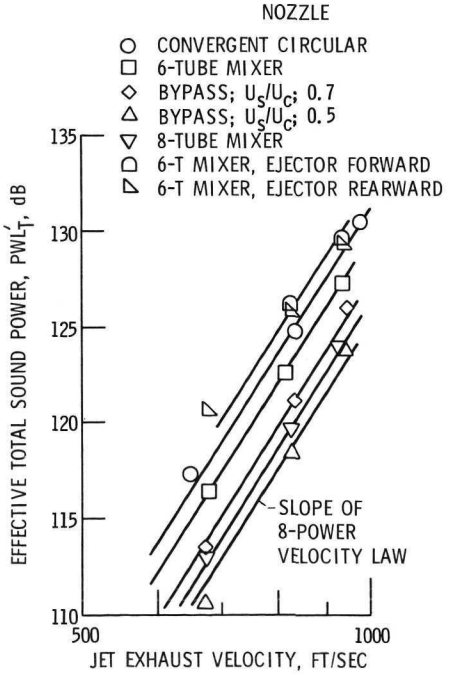

Figure 22. - Effective total sound power as function of jet exhaust (core) velocity for nozzle-wing configurations tested. Zero forward velocity.

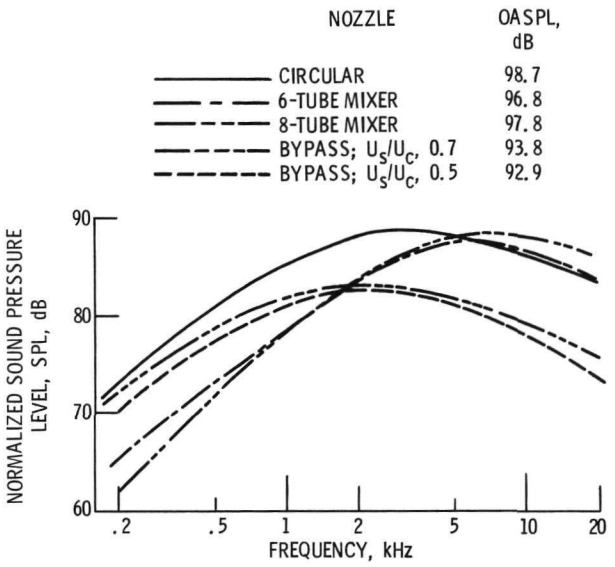

Figure 23. - Sound pressure level spectra for nozzles-only normalized to equal thrust basis. Nominal jet exhaust (core) velocity, 940 ft/sec; zero forward velocity; radiation angle, 90^0.

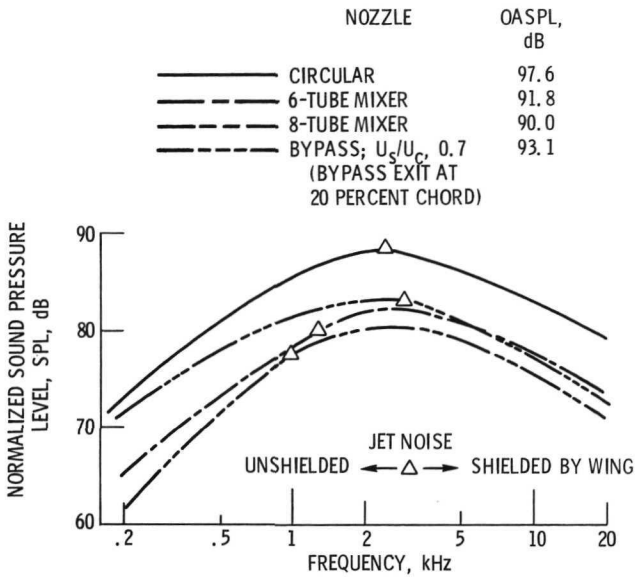

Figure 24. - Sound pressure level spectra for nozzle-wing configurations normalized to equal thrust basis and constant wing chord. Nominal jet exhaust (or core) velocity, 940 ft/sec; zero forward velocity; radiation angle, 90^0.

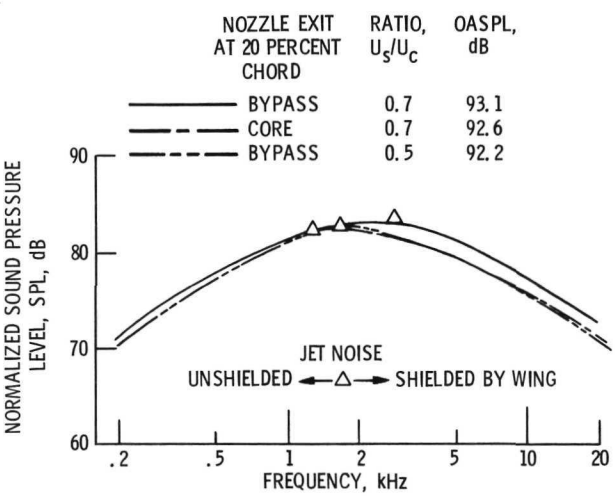

Figure 25. - Sound pressure level spectra for several bypass nozzle-wing configuration variations normalized to equal thrust basis and constant wing chord. Nominal jet core velocity, 940 ft/sec; zero forward velocity; radiation angle, 90^0.

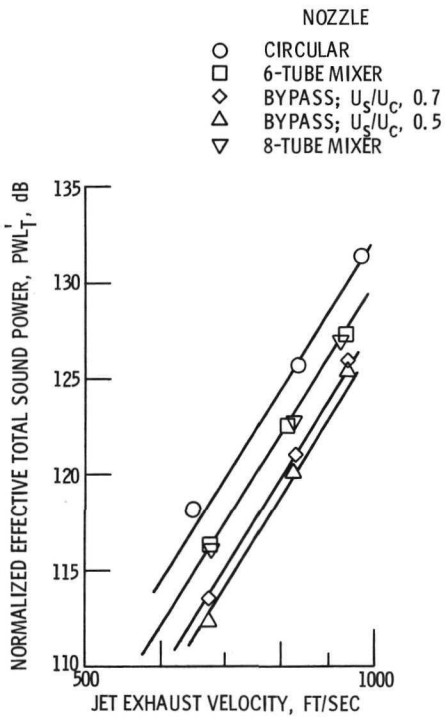

Figure 26. - Total sound power for nozzle-wing configurations normalized to equal thrust basis and constant wing chord. Zero forward velocity.